IET Microwaves, Antennas & Propagation

Research Article

IET Journals
The Institution of Engineering and Technology

Compact dual-band antenna with a lumped capacitor for wireless local area network applications

ISSN 1751-8725
Received on 10th October 2014
Revised on 1st July 2015
Accepted on 21st July 2015
doi: 10.1049/iet-map.2015.0213
www.ietdl.org

Min-Jae Lee[1], *Jung-Ho Ahn*[2], *Young-Sik Kim*[1] ✉

[1]*Department of Computer and Radio Communications Engineering, Korea University, Seoul 136-713, Republic of Korea*
[2]*Samsung Electronics Co., Suwon 443-742, Republic of Korea*
✉ *E-mail: yskim@korea.ac.kr*

Abstract: This study presents a compact dual-band antenna for wireless local area network (WLAN) applications. The proposed antenna consists of small striplines on both sides of a substrate and a lumped capacitor on the top side to reduce the antenna size. As a folded monopole-type resonance is occurred in 5 GHz band, the proposed antenna yields dual-band characteristics. The resonant mechanism is also analysed using the equivalent circuit model. Electric characteristics of the proposed antenna such as radiation patterns, peak gains, and radiation efficiencies, are presented through the simulation and measurement under various conditions. The antenna size is only 5×9 mm^2. The proposed antenna can cover both WLAN bands of 2.4 and 5 GHz.

1 Introduction

A wireless local area network (WLAN) service is attractive because of the non-licensed spectrum, a low cost, and a simple architecture. According to the Institute of Electrical and Electronics Engineers (IEEE) standard, the WLAN frequencies are assigned to 2.4–2.484 GHz for the 802.11b/g standard and 5.15–5.35/5.725–5.825 GHz for the 802.11a standard [1]. Thus, a WLAN antenna may cover the dual or triple band. Another issue is that there is not much room for a WLAN antenna in a mobile handset because many other antennas are equipped for a cellular system, a global positioning system (GPS), a digital multimedia broadcasting system and so on.

A WLAN antenna with the planar monopole-type geometry is very popular because of its simple structure, broad impedance bandwidth, and omni-directional radiation [2–6]. In spite of all the above advantages, the planar monopole antenna is inappropriate for a mobile terminal due to its size. To miniaturise the planar monopole antenna, the planar inverted F antenna (PIFA) has been implemented [7, 8]. Although the PIFA is very usual due to its small size and multiband characteristics, the PIFA has a three-dimensional (3D) scheme. In addition to these, the chip type and L- or E-shaped antennas have been developed [9–11].

In this paper, a compact dual-band antenna with a lumped capacitor for WLAN applications is proposed. The proposed antenna has a dual-band operation, which is the 2.4 GHz band (2.4–2.484 GHz) and 5 GHz band (5.15–5.35/5.725–5.825 GHz). The dual band in the WLAN band is achieved from the loop strips with a tuning capacitor in the lower band and the folded monopole resonance in the upper band. The surface current distribution, equivalent circuit model and parameter study are performed to define electrical characteristics of the proposed antenna. The volume of the proposed antenna is only $5 \times 9 \times 0.8$ mm^3. Radiation characteristics of the proposed antenna such as radiation patterns, peak gains, and radiation efficiencies, have been compared between simulation and experiment. In addition, the effects of a ground size and an antenna position have been investigated.

2 Antenna design

The geometry of the proposed antenna is depicted in Fig. 1. The proposed antenna consists of a radiating loop strip connected with a lumped capacitor on the top ground plane and a meandered stripline on the bottom ground plane. The ground planes are placed on both sides of the substrate to provide actual condition and both planes are electrically connected to each other by metallic through holes. The antenna is designed on a 0.8 mm thick dielectric substrate with a permittivity of 4.4 and a total size of 65×100 mm^2. The antenna is located on the left side of the substrate and x_l away from the upper edge. Its area is $W_{a1} \times L_{a1}$. The antenna is directly fed by a 50 Ω coaxial cable at a point of A. The length and the width of the total substrate are g_l and g_w, respectively. The simulations through the finite element method simulator of high frequency simulator structure (HFSS) [12] and the advanced design system (ADS) simulator [13] have been carried out for antennas and the circuit model, respectively.

The top stripline without a bottom stripline is firstly checked out. Fig. 2 shows the input impedance for three different conditions; open, short, and capacitor terminations. For the short termination, the reactance is rapidly changed from inductance to capacitance crossing the resonant frequency and the resistance is almost infinite at 2.85 GHz. The antenna shows a normal loop antenna characteristic because the anti-resonance is occurred firstly [14]. For the open termination, the reactance is slowly varied from capacitance to inductance. The reactance becomes zero around 5 GHz and the resistance is very small. The resonance may be occurred more than 7 GHz and the antenna operates as a strip monopole antenna. For the capacitor termination, the anti-resonance is being fallen between the short and open terminations. As the capacitance is increased, the impedance characteristic is close to that of the short termination. Each reactance has a zero-cross frequency less than 3 GHz and more than 5 GHz. The resistance is pretty small at a low frequency, while the resistance has an adequate value at a high frequency. It can be stated that the antenna with a proper capacitor termination may well operate in an upper band.

The bottom stripline is adapted to improve in a low band. Similarly, the input impedance for three different conditions; open, short, and capacitor terminations are simulated as shown in Fig. 3. The reflection coefficient is also included. In case of [4, 5], the same bottom scheme is examined, but the former is the short termination and the latter is the open one. The antenna with both terminations yields two anti-resonances in a frequency band of 1–7 GHz. The antenna with the short termination has lower anti-resonant frequencies than that with the open one. In case of

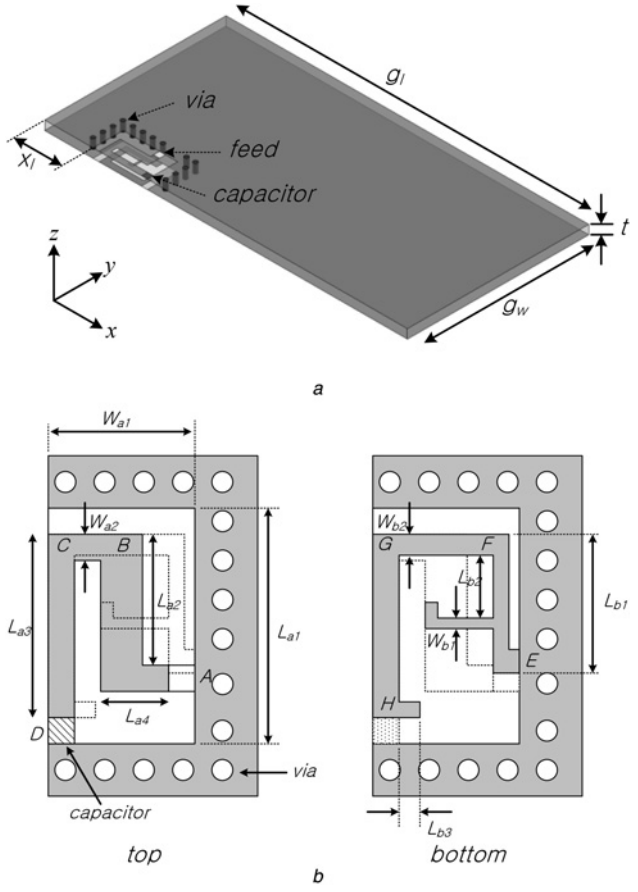

Fig. 1 *Geometry of the proposed antenna*

a General view
b Details

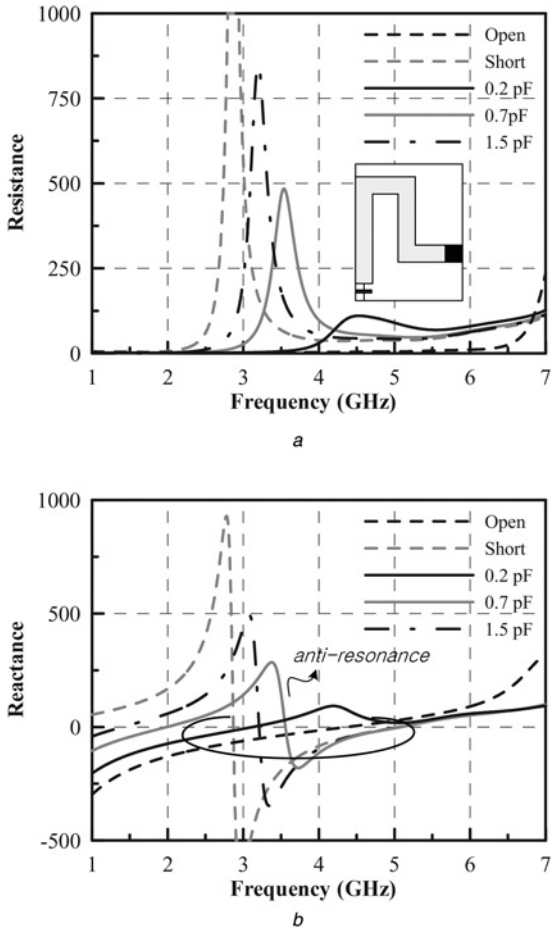

Fig. 2 *Input impedance of the antenna with the top stripline*

a Resistance
b Reactance

[1, 2], different bottom schemes are tested and each top stipline is terminated with a 0.7 pF capacitor. The former is the L-shaped line and the latter is the proposed antenna scheme. Both antennas have an anti-resonance about 4 GHz. The proposed antenna scheme provides a zero-crossing frequency of the reactance at 2.4 GHz. In case of [2, 3], the proposed antenna scheme with different capacitance terminations is compared. The antenna with a capacitance of 0.7 pF shows a higher resonant frequency and a lower peak resistance than the antenna with a 1.5 pF. In Fig. 3*c*, the reflection coefficients behave similarly in the upper band except the antenna with the open termination [5], while the reflection coefficients act differently except the proposed antenna scheme with a 0.7 pF termination [2]. It can be expected that the proposed antenna with a capacitor termination may properly operate in a dual band.

Fig. 4 shows parameter studies. In these parameter studies, the capacitance value is fixed at 0.7 pF. Other parameters are $W_{a1} = 5$ mm, $W_{a2} = 1$ mm, $W_{b1} = 0.3$ mm, $W_{b2} = 0.9$ mm, $L_{a1} = 9$ mm, $L_{a2} = 5$ mm, $L_{a3} = 7$ mm, $L_{a4} = 2$ mm, $L_{b1} = 5.5$ mm, $L_{b2} = 2.2$ mm, and $L_{b3} = 0.8$ mm. Fig. 4*a* shows the reflection coefficients for different L_{a2}, while other parameters are fixed as given above. As L_{a2} is varied, the feeding point, ***A***, is changed. Similarly, Fig. 4*b* shows the reflection coefficients for different L_{b1}. As L_{b1} is varied, the starting point, ***E***, of the meander line is changed. Although the length of the loop is changed with L_{a2} and L_{b1}, the lower resonant frequency is slightly varied. On the other hand, the higher resonance, which is a kind of a folded monopole resonance, is greatly influenced from the loop length and is very sensitive to L_{a2} and L_{b1}. Fig. 4*c* shows that the lower resonant frequency is decreased as L_{b3} is increased. The increase of L_{b3} can result in C_l and L_{l2} increase in Fig. 7.

The position of a WLAN antenna cannot be freely placed in a mobile terminal because of a limited space and other devices. To find an antenna position effect, the distance between the ground plane edge and the antenna is examined. Fig. 5 shows the reflection coefficients for different x_l which is the distance between the ground plane edge and the antenna. As the distance is varied, the resonant frequency in the upper band is also changed because the currents flow on both of the top sides of the ground planes (see Fig. 6*b*). The distances of 5 and 65 mm yield a similar impedance bandwidth of −7.3 dB (voltage standing wave ratio – VSWR = 2.5), while other distances have −6 dB impedance bandwidth (VSWR = 3.0), that is acceptable for mobile applications [15–17]. The variations of resonant frequencies in the lower and higher bands are 1.2 and 4.8% with respect to each centre frequency, respectively. It may be stated that the position of the proposed antenna is more influenced on the resonant frequency in the higher band.

The resonances of the proposed antenna are generated at the 2.4 and 5 GHz bands. The simulated surface currents at 2.45 and 5.45 GHz are shown in Fig. 6. The white triangle denotes a peak value, whereas the dark one denotes almost no surface current. The feeding current flows in both directions of the top stripline and the top ground plane through the tuning capacitor. These surface currents are nulled between ***C*** and ***D***. The coupled currents on the bottom stripline and the bottom ground plane flow in on direction and are nulled at the disconnected point, ***H***. As the tuning capacitance is increased, the null point is changed and the resonant frequency is decreased because the electrical length is varied, as shown in Fig. 3. Each current distribution of the top and bottom planes is similar to be a $\lambda/2$ resonant loop. It may be noted that the difference (opposite direction) and sum (same direction) of two currents can contribute to the antenna radiation. The current distribution at 5.45 GHz is illustrated in Fig. 6*b*. The currents on the top (***A***–***C***) and the bottom (***E***–***G***) strips are large and flow in

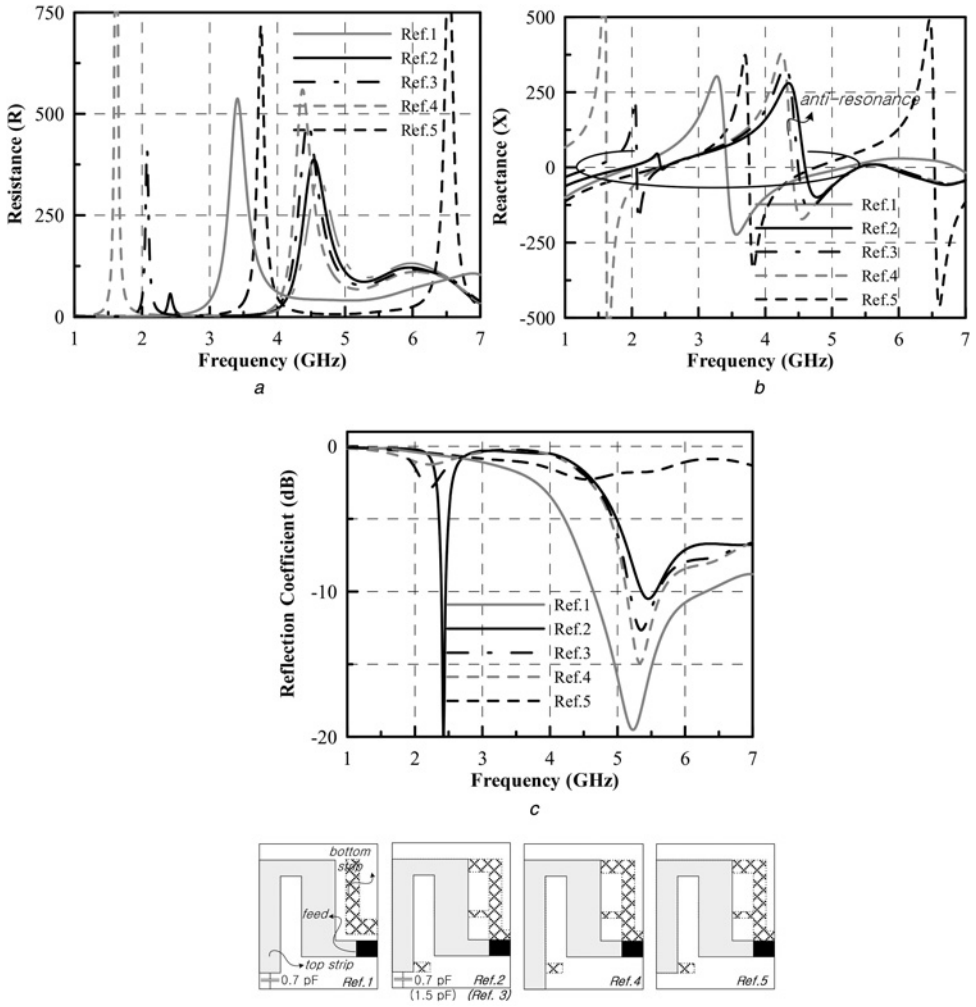

Fig. 3 *Input impedance and reflection coefficient of the antenna with the top and bottom striplines*

a Resistance
b Reactance
c Reflection coefficient

the same direction. At 5.45 GHz, the antenna acts as a folded monopole, whose electrical length is 0.22λ.

The equivalent circuit model is also illustrated in Fig. 7*a*. In Fig. 7*a*, C_l and L_{l2} are capacitance and inductance of the loop resonance, respectively. C_{cap} is the tuning capacitance, and L_{l1} is the inductance of the stripline. The circuit elements of the folded monopole resonance are C_f and L_f. The parasitic resonance, which consists of C_p, L_p, and R_p, is occurred at a length of 0.42λ of the bottom stripline. This kind of resonance can contribute to widening the bandwidth in the higher band. The C_g is a gap capacitance between the stripline near the feeding and the circumferential ground plane. The reflection coefficient and impedance of the equivalent circuit model are derived through the ADS simulator, and are compared with those of the HFSS simulator. As shown in Figs. 7*b* and *c*, the results of the circuit model are good agreed with those of the HFSS simulator.

3 Experimental results

The proposed antenna is implemented on a 0.8 mm thick FR-4 substrate with a dielectric constant of 4.4 and an overall size of 65×100 mm^2 ($g_w \times g_l$). The design parameters are the same as those given in Section 2. As a capacitance value of 0.7 pF is not available, a lumped capacitor of 0.68 pF manufactured by YAGEO Corp. is utilised [18]. The antenna position, x_l, is 12 mm and the diameter of metallic through holes is 0.7 mm.

The simulated and measured reflection coefficients are presented in Fig. 8*a*. As mentioned before, the impedance bandwidth of −7.3 dB is usually accepted to design an antenna for WLAN services, although the −10 bandwidth is seldom reported [15–17, 19, 20]. The −7.3 dB bandwidths in the lower and higher bands are 90 MHz (2.395 – 2.485 GHz) and more than 725 MHz (higher than 5.1 GHz), respectively. The simulated results agree well with the measured ones.

The 3D radiation patterns of the proposed antenna have been measured in a $5.5 \times 5.5 \times 5$ m^3 anechoic chamber. As shown in Fig. 8*b*, radiation efficiencies and peak gains in 2.4 GHz band are better than 42% and 1.1 dBi, respectively. Since the surface currents on the top and bottom strips (***A***–***C*** and ***E***–***G***) flow along the opposite direction, it can be expected that the radiation efficiency and peak gain may be small. However, the marginal efficiency of an antenna which is operated in the cellular band is about 40%. In general, the required antenna efficiency of a WLAN antenna is usually less than that of a cellular antenna [21]. Thus, the efficiency of the proposed antenna is good enough to utilise. At 5 GHz band, the radiation efficiency and the peak gain are 90.08% and 6.25 dBi, respectively. The radiation efficiency and the peak gain obtained from the simulation are better than those from the experiment because the measured peak gain includes the ohmic losses of a coaxial cable, a substrate, and a lumped capacitor [17]. The measured peak gain is the same as the realised gain in [22]. In 5.95 GHz, the measured results are slightly better than the simulated ones because of the better reflection coefficient.

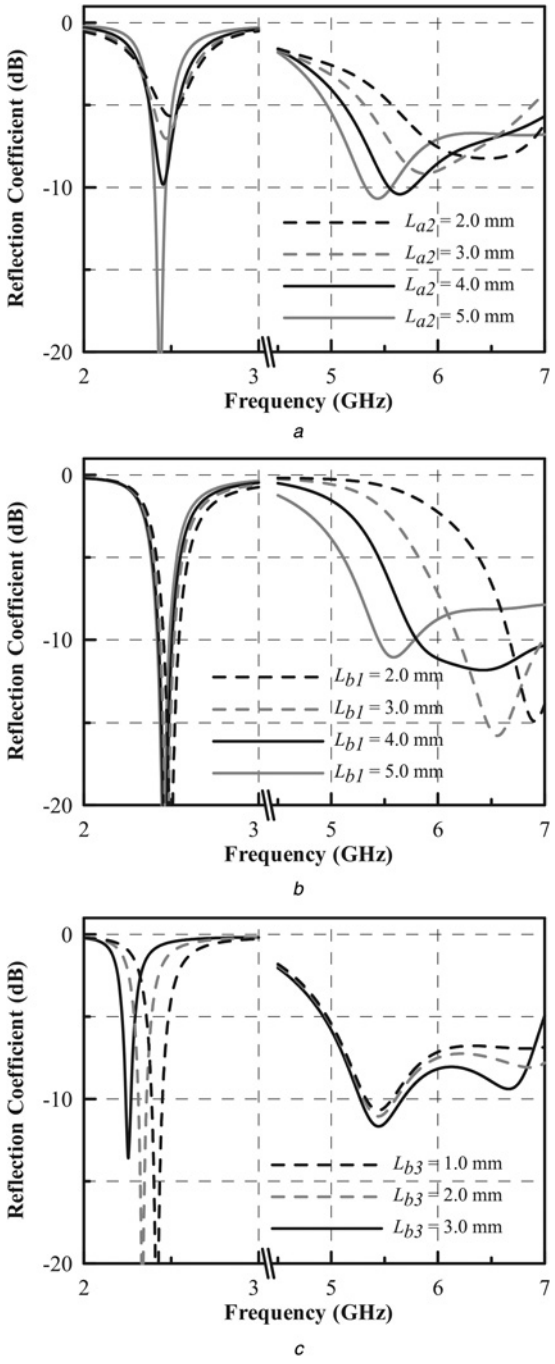

Fig. 4 *Parameter studies*

a L_{a2}
b L_{b1}
c L_{b3}

According to the data sheet of the capacitor, the capacitor has a dissipation factor of 0.0025 at 1 MHz [18, 23].

Fig. 9 shows the simulated and measured radiation patterns at 2.45 and 5.45 GHz, respectively. As the proposed antenna is encircled by the ground plane and the loop shape is not symmetric, the radiation pattern of the 2.45 GHz is tilted to 45°. Although the radiation patterns are distorted in the *y*-direction due to the asymmetric antenna shape, the proposed antenna nearly has an omni-directional pattern at 5.45 GHz. The measured radiation patterns are agreed well with the simulated ones at both frequencies.

Table 1 is summed up to compare an antenna size reduction, VSWR, measured efficiency, and gain with other published WLAN antennas. It can be noted that the proposed antenna has performed pretty well, especially in the efficiency and gain.

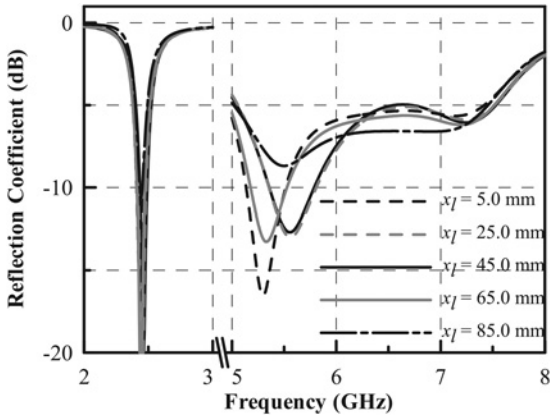

Fig. 5 *Simulated reflection coefficients as variation of* x_l

The VSWR is moderate among others, but the size is the smallest. The proposed antenna has a 2.5:1 ($S_{11} = -7.4$ dB), while the others have 2:1 ($S_{11} = -9.5$ dB) and 3:1 ($S_{11} = -6.0$ dB).

The ground size of the antenna becomes sometimes larger than the optimally designed size when the antenna is installed with other devices such as a universal serial bus (USB) dongle and a laptop/notebook PC (personal computer) for WLAN services. The laptop has an enough space for an antenna and a ground plane. If a USB dongle with an antenna is connected to a PC, the circuit board of the PC acts as the ground plane of the antenna.

In this paper, the ground size is extended to 200 × 200 mm^2. That is a least size for a notebook PC and a USB dongle. Fig. 10 shows the

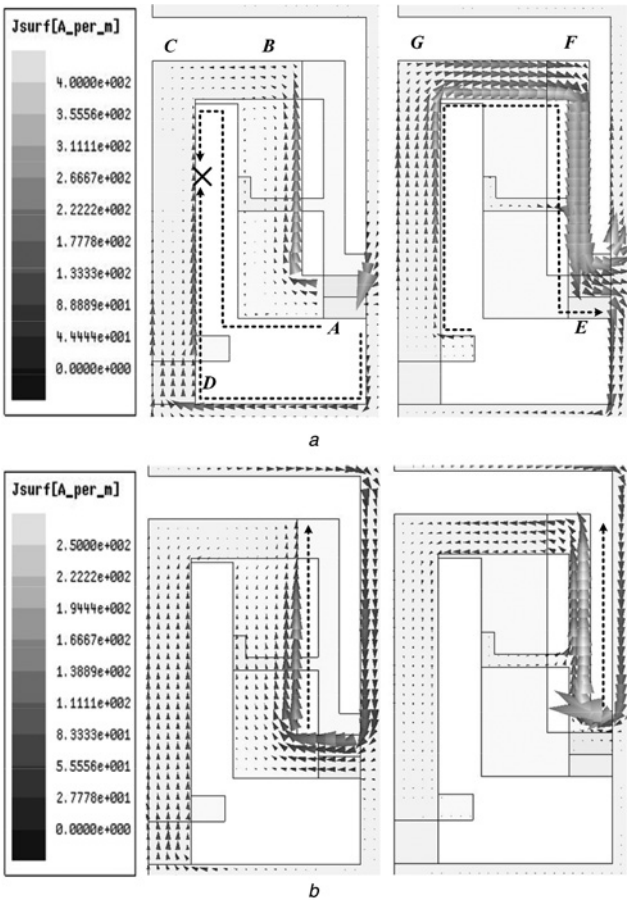

Fig. 6 *Simulated surface current distributions*

a 2.45 GHz
b 5.45 GHz

IET Microw. Antennas Propag., 2015, Vol. 9, Iss. 15, pp. 1747–1754

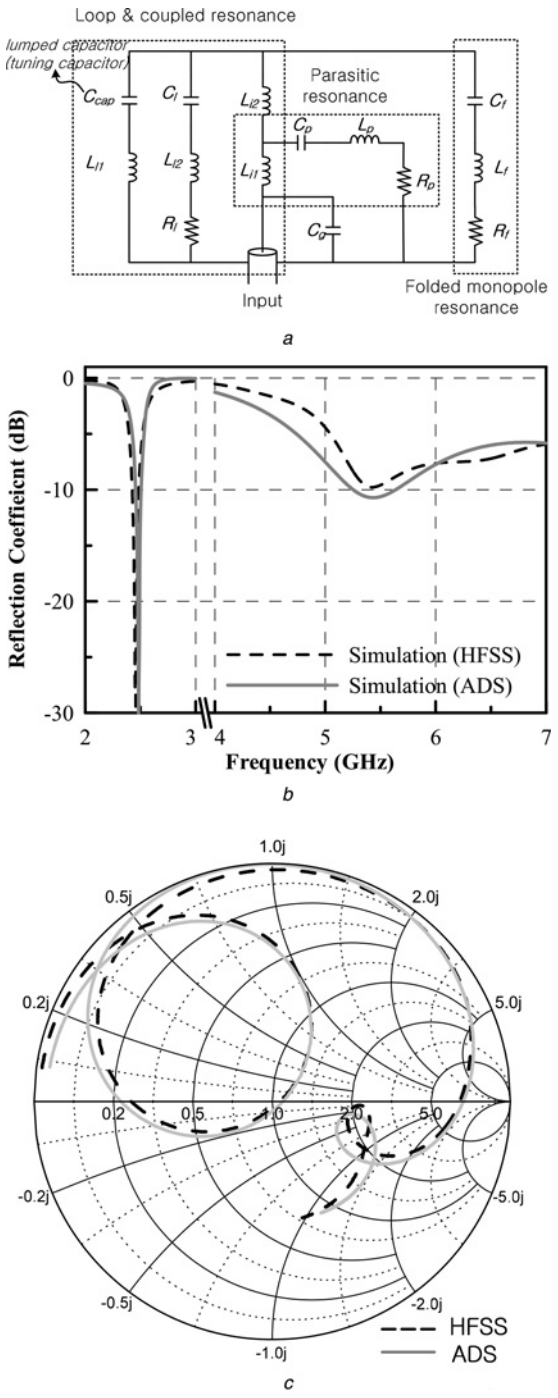

Fig. 7 *Equivalent circuit and simulated results*

a Equivalent circuit model
b Simulated reflection coefficient
c Simulated Smith chart

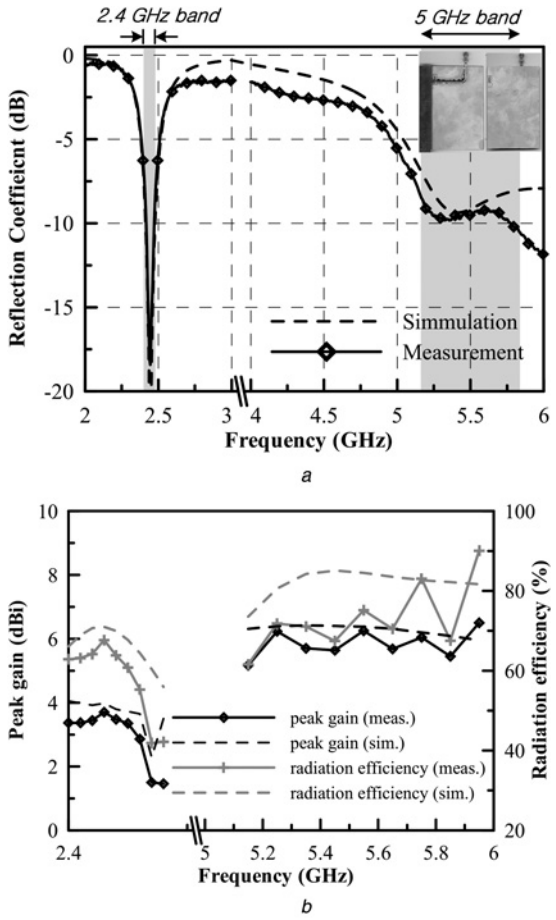

Fig. 8 *Simulated and measured results of the proposed antenna*

a Reflection coefficients
b Peak gain and radiation efficiency

simulated and measured reflection coefficients for different ground sizes. The proposed antenna yields reflection coefficients of below −7.3 dB at both bands. The resonant frequency at the lower band is not much changed due to a relatively large wavelength.

In practical circumstances, an antenna may be laid out with a nearby large conductor such as a large LCD mounted on a metal plate, because the display area of a smart phone is getting large nowadays. The configuration of a nearby conductor is depicted in Fig. 11*a*, because the ground plane of the proposed antenna can be placed on either a top or bottom side. d_{top} and d_{bottom} are the distances from the proposed antenna. In the simulation, the nearby conductor is assumed to be a perfect electric conductor (PEC). The antenna and the upper side region are cut out of a PEC to radiate properly. Figs. 11*b* and *c* show the impedance versus the separation normalised with the resonant wavelength. R_{freqency} and $X_{\text{frequency}}$ are the resistance and the reactance at each resonant frequency without the PEC, respectively. As the total current on the antenna is comprised in the induced current due to the fields reflected from the PEC, the impedance may be altered [24–27]. As shown in Fig. 11, the PEC has a little effect on the antenna impedance at 2.45 GHz because the PEC size is small with respect to the wavelength. At 5.4 GHz, the antenna reactance has some fluctuations and zero at two places. The antenna at a high frequency is more deviated than that at a low frequency due to a short wavelength.

Figs. 12*a* and *b* show the simulated and measured reflection coefficients for different distances between the proposed antenna and the single PEC. Once the distance is zero, the PEC is shorted with the ground plane of the proposed antenna. Thus, the minimum distance is 1 mm in this paper. Furthermore, the ROHACELL foam with a dielectric constant of 1.04 – 1.05 (2.5 – 5 GHz), which is made by Evonik Ind. [28], is inserted between the proposed antenna and the PEC. In Figs. 12*a* and *b*, the lower resonant frequency is not much affected for both cases. The higher resonant frequency is slightly decreased as the distance is increased for both cases. In the upper band of Figs. 12*a* and *b*, the extra resonance at both of a distance of 5 mm is occurred about 6.3 GHz. It may be noted that the measured reflection coefficients with the PEC either above or under the antenna are better than the simulated ones in the upper band. The simulated and measured peak gains and radiation efficiencies for above and bottom PECs with a distance of 5 mm are shown in Figs. 12*c* and *d*. In the 2.4 GHz band, radiation efficiencies of both cases are similar to the

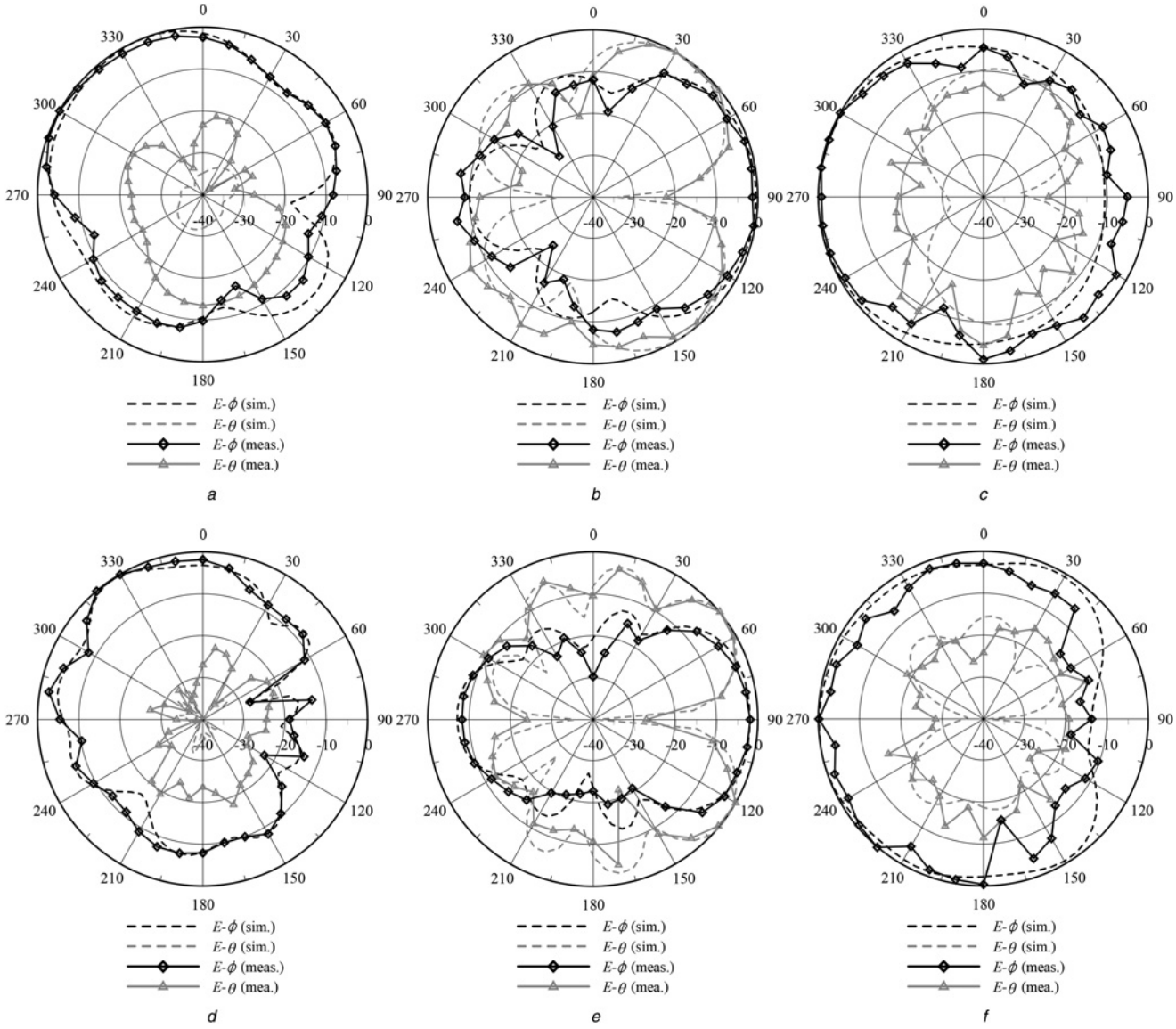

Fig. 9 *Simulated and measured radiation patterns*

a *xy*-plane at 2.45 GHz
b *zx*-plane at 2.45 GHz
c *zy*-plane at 2.45 GHz
d *xy*-plane at 5.45 GHz
e *zx*-plane at 5.45 GHz
f *zy*-plane at 5.45 GHz

case of without the PEC. In the 5 GHz band, the slope of the peak gain is steeper than that of the antenna without the PEC because the PEC acts as the reflector. The measured peak gain overtakes

Table 1 Comparison of the antenna size reduction, VSWR and measured efficiencies with other WLAN antennas

Ref	Antenna size reduction ([ref.]/ proposed antenna) and service bands	VSWR	Measured efficiency		Peak gain	
			Max., %	Min., %	Max., dBi	Min., dBi
[2]	2500%/WLAN	2: 1	69	42	–	–
[9]	202.02%/WLAN	2: 1	60	52	2.8	1
[11]	888.89%/WLAN	2: 1	89	52	2.32	−0.9
[19]	1000%/WLAN	2.5: 1	50.1	31.6	–	–
[20]	GSM/GPS/PCS/ UMTS/WLAN	3: 1	39–37	34.1	0.5	−0.19
proposed antenna	100%	2.5: 1	90.08	42	6.25	1.1

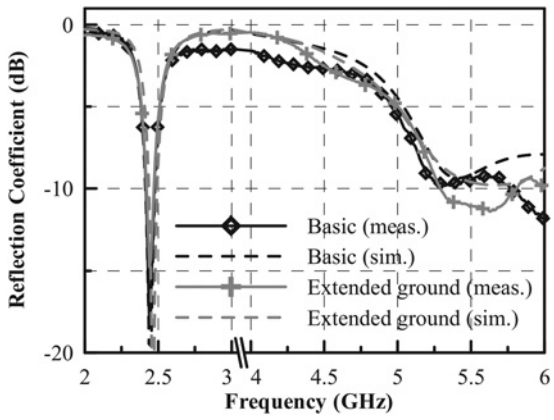

Fig. 10 *Simulated and measured reflection coefficients for different ground sizes*

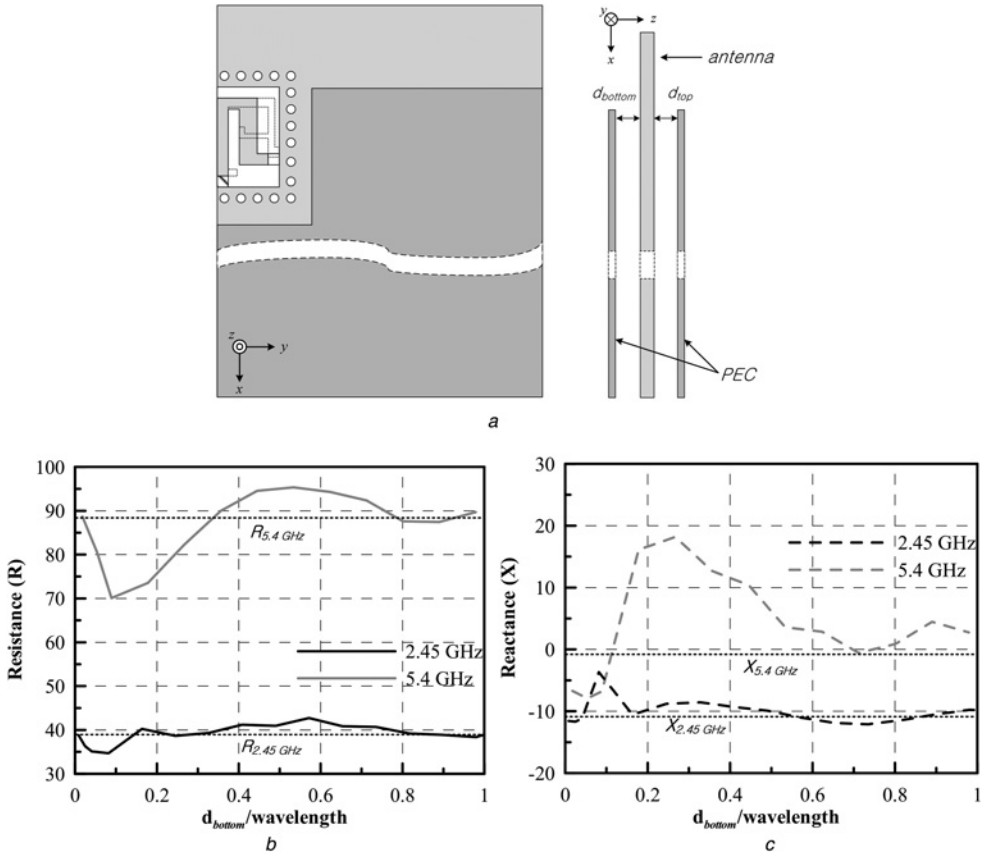

Fig. 11 *Experimental setting and simulated impedance of the antenna with the PEC placed under the antenna*

a Front and side views
b Resistance
c Reactance

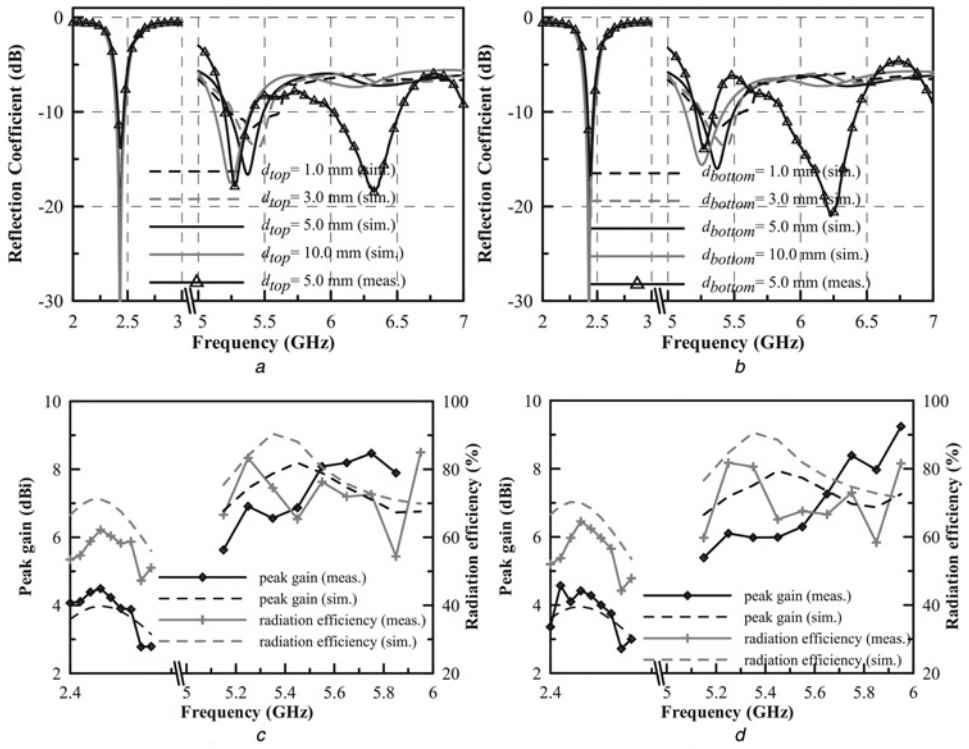

Fig. 12 *Simulated and measured results*

a Reflection coefficient of the antenna with the PEC placed above the antenna
b Reflection coefficient of the antenna with the PEC placed under the antenna
c Peak gain and radiation efficiency of the antenna with the PEC placed above the antenna
b Peak gain and radiation efficiency of the antenna with the PEC placed under the antenna

the simulated ones due to the better reflection coefficient. Though the radiation efficiency is slightly reduced, the overall antenna performance is acceptable for WLAN applications.

4 Conclusion

In this paper, a compact dual-band antenna with a lumped capacitor for WLAN applications is presented. The effects of the ground size and the metal plate with an LCD have been studied. The proposed antenna is suitable to be installed in the devices such as a mobile phone, a USB dongle and a laptop for WLAN services in 2.4 and 5 GHz bands.

5 References

1 P802.11: 'IEEE Standard for Wireless LAN Medium Access Control (MAC) and Physical Layer (PHY) Specifications', April 2012
2 D'Souza, R., Gupta, R.K.: 'Printed dual band WLAN antenna'. Proc. IEEE Int. Conf. Electronics Information Technology, Miami, USA, May 2006, pp. 539–543
3 Basaran, S.C., Erdemil, Y.E.: 'A dual-band split ring monopole antenna for WLAN applications', *Microw. Opt. Technol. Lett.*, 2009, **51**, (11), pp. 2685–2688
4 Hsie, C., Chiu, T.: 'Dual-band antenna design using a dual-feed monopole slot', *IET Microw. Antennas Propag.*, 2011, **5**, (12), pp. 1502–1507
5 Elghannai, E.A., Rojas, R.G.: 'Design of USB dongle antenna for WLAN applications using theory of characteristic modes', *Electron. Lett.*, 2014, **50**, (4), pp. 249–251
6 Basaran, S.C., Olgun, U., Sertel, K.: 'Multiband monopole antenna with complementary split-ring resonators for WLAN and WiMAX applications', *Electron. Lett.*, 2013, **49**, (10), pp. 636–638
7 Wang, H., Zheng, M.: 'An internal triple-band WALN antenna', *IEEE Antenna Wirel. Propag. Lett.*, 2011, **10**, pp. 569–572
8 Cho, Y.J., Shin, Y.S., Park, S.O.: 'Internal PIFA for 2.4/5 GHz WLAN applications', *Electron. Lett.*, 2006, **42**, (1), pp. 8–10
9 Chien, H.-Y., Sim, C.-Y.-D., Lee, C.-H.: 'Compact size dual-band antenna printed on flexible substrate for WLAN operation'. Proc. Int. Symp. Antennas and Propagation, Nagoya, Japan, October 2012
10 Wong, K.-L., Chang, C.-H.: 'WLAN chip antenna mountable above system ground plane of a mobile devices', *IEEE Trans. Antennas Propag.*, 2005, **53**, (11), pp. 3496–3499
11 Sun, X.L., Liu, L., Cheung, S.W., *et al.*: 'Dual-band antenna with compact radiator for 2.4/5.2/5.8 GHz WLAN applications', *IEEE Trans. Antennas Propag.*, 2012, **60**, (12), pp. 5924–5931
12 HFSS User Manual, Ansys Inc., Pennsylvania, US, 2013
13 ADS 2005A, Agilent Technologies Inc., California, US, 2005
14 McKinley, A.F., White, T.P., Catchpole, K.R.: 'Theory of the circular closed loop antenna in the terahertz, infrared, and optical regions', *J. Appl. Phys.*, 2013, **114**, (044317), pp. 1–10
15 Chu, F.-H., Wong, K.-L.: 'Internal coupled-fed dual-loop antenna integrated with a USB connector for WWAN/LTE mobile handset', *IEEE Trans. Antennas Propag.*, 2011, **59**, (11), pp. 4215–4221
16 Antenna Fundamentals: Technical Brief, AT&T Inc., Texas, US, 2009
17 Wong, K.-L., Tsai, C.-Y.: 'Small-size stacked inverted-F antenna with two hybrid shorting strips for the LTE/WWAN tablet devices', *IEEE Trans. Antennas Propag.*, 2014, **62**, (8), pp. 3962–3969
18 Data Sheet: Surface-Mount Ceramic Multilayer Capacitors, YAGEO Corp., New Taipei City, TW, 2013
19 Bancroft, R.: 'A commercial perspective on the development and integration of an 802.11 a/b/g hiperlan/WLAN antenna into laptop computers', *IEEE Antennas Propag. Mag.*, 2006, **48**, (4), pp. 12–18
20 Li, Y., Zhang, Z., Zheng, J., *et al.*: 'Compact heptaband reconfigurable loop antenna for mobile handset', *IEEE Antenna Wirel. Propag. Lett.*, 2011, **10**, pp. 1162–1165
21 Chen, Z.N.: 'Antennas for portable devices' (John Wiley & Sons, 2007, 1st edn.)
22 IEEE Antenna and Propagation Society: 'IEEE Standards for Definitions of Terms for Antennas', 2014
23 Bahl, I.: 'Lumped elements for RF and microwave circuits' (Artech House, 2003, 1st edn.)
24 Proctor, R.F.: 'Input impedance of horizontal dipole aerials at low heights above the ground'. Proc. IEE Radio and Communications Engineering, May 1950, vol. 97, no. 47, pp. 188–190
25 Kraus, J.D., Marhrfka, R.J.: 'Antennas for all applications' (McGraw-Hill, 2003, 3rd edn.)
26 Balanis, C.A.: 'Antenna theory' (John Wiley & Sons, 2005, 3rd edn.)
27 Lindell, I.V., Alanen, E., Mannersalo, K.: 'Exact image method for impedance computation of antennas above the ground', *IEEE Trans. Antennas Propag.*, 1985, **33**, (9), pp. 937–945
28 Dielectric Properties, EVONIK Ind., Essen, DE, 2011